Kite aerodynamics in the `awebox`

R. Leuthold, J. De Schutter, T. Bronnenmeyer, M. Diehl

March 6, 2020

1 Introduction

Our goal is to model the aerodynamic force on a particular kite, in a way that this model can be used in the `awebox`.

In this document, we:

- (Section 2) define some aspects of aerodynamics that will allow the determination of the force to procede more smoothly;
- (Section 3) apply those definitions to create a procedure for determining the aerodynamic force on a kite; and
- (Section 4) explain how an `awebox` user can interact with the code to model the kite aerodynamics.

(Note to the reader: since any model can only be useful when its assumptions are valid, we have here highlighted the assumptions to make them immediately visible to you.)

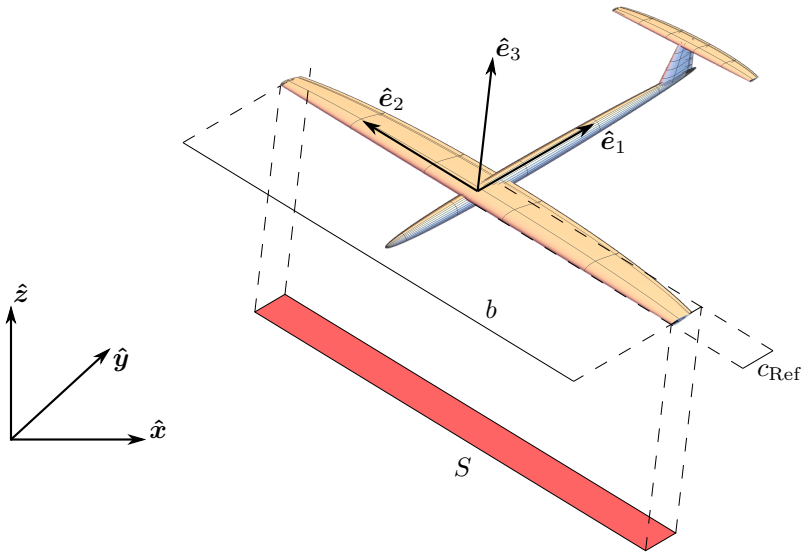

Figure 1: The kite, whose orientation is described by the kite-fixed reference frame, is flying in the earth-fixed reference frame. The total planform area of the kite is S - which, with the known span b, prescribes the mean aerodynamic chord c_{Ref}.

2 Naming conventions and reference frames

Our goal here is to define some terminology and reference frames that will aid us to find the aerodynamic force acting on the kite. In this section, we'll separate these conventions according to topics pertaining to:

- (Section 2.1) the earth-fixed reference frame,
- (Section 2.2) the kite,
- (Section 2.3) the apparent velocity,
- (Section 2.4) the induced velocity,
- (Section 2.5) the effective velocity,
- (Section 2.6) the force vector and its projections, and
- (Section 2.7) the aerodynamic stability derivatives.

2.1 the earth-fixed reference frame

The earth-fixed reference frame is described by three axis: $\hat{\boldsymbol{x}}$, which is along the dominant wind direction; $\hat{\boldsymbol{y}}$ which points horizontally to the side; and $\hat{\boldsymbol{z}}$ which points upwards against gravity.

We can use the direction cosine matrix $\underline{\boldsymbol{R}}_i$ to return a vector $\boldsymbol{v}_i$ in the reference frame i to the earth-fixed reference frame E, according to $\boldsymbol{v}_{\mathrm{E}} = \underline{\boldsymbol{R}}_i \boldsymbol{v}_i$.

2.2 the kite and the kite-fixed reference frame

The kite has a known planform area S and wing-span b. Together, these define a mean-aerodynamic-chord c_{Ref}, with which the rectangular area $(b)(c_{\mathrm{Ref}}) = S$. (Notice that this chord doesn't say anything about the chord of the wing at root or tip!) Then, we can define a helpful ratio called the *aspect ratio* as $\mathit{AR} = b/c_{\mathrm{Ref}} = b^2/S$.

The kite has three principle axes. First, we have $\hat{\boldsymbol{e}}_1$ which points from the nose to the tail, or - alternatively stated - chordwise, from leading edge to trailing edge. Second, we have $\hat{\boldsymbol{e}}_2$ which points along the kite's span. Third, we have $\hat{\boldsymbol{e}}_3$ which points upwards. These three axes give us a *kite-fixed reference*

frame[1], described by the direction cosine matrix $\underline{\boldsymbol{R}}_{\mathrm{K}} = \left(\hat{\boldsymbol{e}}_1, \hat{\boldsymbol{e}}_2, \hat{\boldsymbol{e}}_3\right)$. We'll locate the origin $\boldsymbol{O}_{\mathrm{K}}$ of this reference frame at the aerodynamic center of the kite.

The kite, and the kite-fixed reference frame are shown in Figure 1.

2.3 the apparent velocity

The *apparent velocity* is the relative velocity of the kite, not including the changes to the flow-field caused by induction. That is, for a free-stream velocity $\boldsymbol{u}_\infty$, and the motion of the kite $\dot{\boldsymbol{q}}_{\mathrm{K}}$, we define the apparent velocity as:

$$\boldsymbol{u}_{\mathrm{a}} = \boldsymbol{u}_\infty - \dot{\boldsymbol{q}}_{\mathrm{K}} \tag{1}$$

Based on the apparent velocity and the span, we have an *apparent-velocity reference frame*, described by the direction cosine matrix $\underline{\boldsymbol{R}}_{\mathrm{a}} = \left(\hat{\boldsymbol{D}}_{\mathrm{a}}, \hat{\boldsymbol{S}}_{\mathrm{a}}, \hat{\boldsymbol{L}}_{\mathrm{a}}\right)$, where:

$$\hat{\boldsymbol{D}}_{\mathrm{a}} = \frac{\boldsymbol{u}_{\mathrm{a}}}{\|\boldsymbol{u}_{\mathrm{a}}\|_2}, \qquad \hat{\boldsymbol{L}}_{\mathrm{a}} = \frac{\boldsymbol{u}_{\mathrm{a}} \times \hat{\boldsymbol{e}}_2}{\left\|\boldsymbol{u}_{\mathrm{a}} \times \hat{\boldsymbol{e}}_2\right\|_2}, \qquad \hat{\boldsymbol{S}}_{\mathrm{a}} = \frac{\hat{\boldsymbol{L}}_{\mathrm{a}} \times \hat{\boldsymbol{D}}_{\mathrm{a}}}{\left\|\hat{\boldsymbol{L}}_{\mathrm{a}} \times \hat{\boldsymbol{D}}_{\mathrm{a}}\right\|_2}. \tag{2}$$

The angle between the projection of the apparent velocity on the plane containing $\hat{\boldsymbol{e}}_1$ and $\hat{\boldsymbol{e}}_3$, and $\hat{\boldsymbol{e}}_1$ is the *apparent angle-of-attack* α_{a}; the angle between the projection of the apparent velocity on the plane containing $\hat{\boldsymbol{e}}_1$ and $\hat{\boldsymbol{e}}_2$, and $\hat{\boldsymbol{e}}_1$ is the *apparent side-slip angle* β_{a}. With a small angle approximation, we have:

$$\alpha_{\mathrm{a}} = \frac{\boldsymbol{u}_{\mathrm{a}}^\top \hat{\boldsymbol{e}}_3}{\left|\boldsymbol{u}_{\mathrm{a}}^\top \hat{\boldsymbol{e}}_1\right|}, \qquad \beta_{\mathrm{a}} = \frac{\boldsymbol{u}_{\mathrm{a}}^\top \hat{\boldsymbol{e}}_2}{\left|\boldsymbol{u}_{\mathrm{a}}^\top \hat{\boldsymbol{e}}_1\right|}, \tag{3}$$

where the chord-wise component of the velocity had better be positive to avoid significant flow separation.

2.4 the induced velocity

The *induced velocity* $\boldsymbol{u}_{\mathrm{i}}$ is the velocity-field induced by the vortices within the modelled universe.

2.5 the effective velocity

The *effective velocity* is the relative velocity of the kite, including the changes to the flow-field caused by induction. That is, for an induced velocity $\boldsymbol{u}_{\mathrm{i}}$, the effective velocity can be found with:

$$\boldsymbol{u}_{\mathrm{e}} = \boldsymbol{u}_{\mathrm{a}} + \boldsymbol{u}_{\mathrm{i}}. \tag{4}$$

Based on the effective velocity and the span, we have an *effective-velocity reference frame*, described by the direction cosine matrix $\underline{\boldsymbol{R}}_{\mathrm{e}} = \left(\hat{\boldsymbol{D}}_{\mathrm{e}}, \hat{\boldsymbol{S}}_{\mathrm{e}}, \hat{\boldsymbol{L}}_{\mathrm{e}}\right)$, where:

$$\hat{\boldsymbol{D}}_{\mathrm{e}} = \frac{\boldsymbol{u}_{\mathrm{e}}}{\|\boldsymbol{u}_{\mathrm{e}}\|_2}, \qquad \hat{\boldsymbol{L}}_{\mathrm{e}} = \frac{\boldsymbol{u}_{\mathrm{e}} \times \hat{\boldsymbol{e}}_2}{\left\|\boldsymbol{u}_{\mathrm{e}} \times \hat{\boldsymbol{e}}_2\right\|_2}, \qquad \hat{\boldsymbol{S}}_{\mathrm{e}} = \frac{\hat{\boldsymbol{L}}_{\mathrm{e}} \times \hat{\boldsymbol{D}}_{\mathrm{e}}}{\left\|\hat{\boldsymbol{L}}_{\mathrm{e}} \times \hat{\boldsymbol{D}}_{\mathrm{e}}\right\|_2}. \tag{5}$$

The angle between the projection of the effective velocity on the plane containing $\hat{\boldsymbol{e}}_1$ and $\hat{\boldsymbol{e}}_3$, and $\hat{\boldsymbol{e}}_1$ is the *effective angle-of-attack* α_{e}; the angle between the projection of the effective velocity on the plane containing $\hat{\boldsymbol{e}}_1$ and $\hat{\boldsymbol{e}}_2$, and $\hat{\boldsymbol{e}}_1$ is the *effective side-slip angle* β_{e}. With a small angle approximation, we have:

$$\alpha_{\mathrm{e}} = \frac{\boldsymbol{u}_{\mathrm{e}}^\top \hat{\boldsymbol{e}}_3}{\left|\boldsymbol{u}_{\mathrm{e}}^\top \hat{\boldsymbol{e}}_1\right|}, \qquad \beta_{\mathrm{e}} = \frac{\boldsymbol{u}_{\mathrm{e}}^\top \hat{\boldsymbol{e}}_2}{\left|\boldsymbol{u}_{\mathrm{e}}^\top \hat{\boldsymbol{e}}_1\right|}, \tag{6}$$

[1] aka. *body-fixed reference frame* in this specific context

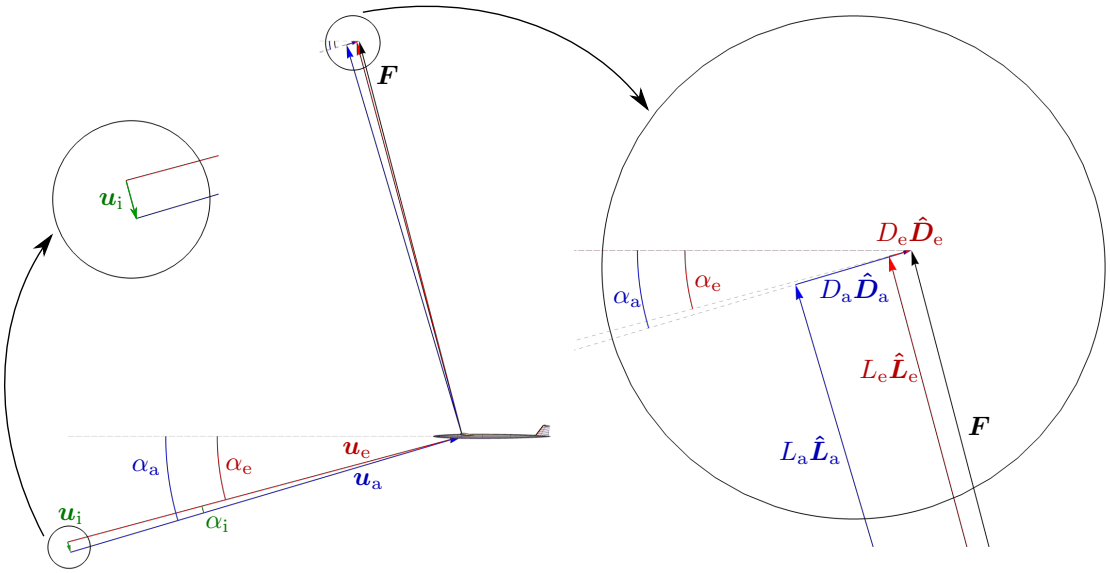

Figure 2: We can project the aerodynamic force $\boldsymbol{F}$ in the apparent-velocity reference frame (blue), or in the effective velocity reference frame (red), resulting in different contributions from lift L_j and drag D_j. The apparent- and effective- references frames are rotated away from each other by the induced angle-of-attack α_i. This means that $\hat{\boldsymbol{D}}_\mathrm{a}$ is not parallel to $\hat{\boldsymbol{D}}_\mathrm{e}$.

where the chord-wise component of the velocity had better be positive to avoid significant flow separation.

Then, the *induced angle of attack* is the difference between the apparent and effective angles-of-attack:

$$\alpha_\mathrm{i} = \alpha_\mathrm{a} - \alpha_\mathrm{e}. \tag{7}$$

The effective- velocity and -angle-of-attack, as well as the induced angle-of-attack are shown in Figure 2.

2.6 the aerodynamic force vector and its projections

For a particular instant, with specific current and historical flight conditions, the aerodynamic force vector F acting on the kite is unique. But, this force can be projected according to an infinite number of reference frames. That is:

$$\boldsymbol{F} = F_\mathrm{x}\hat{\boldsymbol{x}} + F_\mathrm{y}\hat{\boldsymbol{y}} + F_\mathrm{z}\hat{\boldsymbol{z}} = F_\mathrm{A}\hat{\boldsymbol{e}}_1 + F_\mathrm{Y}\hat{\boldsymbol{e}}_2 + F_\mathrm{N}\hat{\boldsymbol{e}}_3 = D_\mathrm{a}\hat{\boldsymbol{D}}_\mathrm{a} + S_\mathrm{a}\hat{\boldsymbol{S}}_\mathrm{a} + L_\mathrm{a}\hat{\boldsymbol{L}}_\mathrm{a} = D_\mathrm{e}\hat{\boldsymbol{D}}_\mathrm{e} + S_\mathrm{e}\hat{\boldsymbol{S}}_\mathrm{e} + L_\mathrm{e}\hat{\boldsymbol{L}}_\mathrm{e}. \tag{8}$$

We can non-dimensionalize these forces by using a product of the dynamic pressure $q_j = (1/2\rho {u_j}^2)$ for $j \in \{\mathrm{a}, \mathrm{e}\}$, and the planform kite area S. For the two reference frames defined by velocities, this defining velocity should be used to determine the dynamic pressure. For the two reference frames that are fixed to objects, the velocity used in the dynamic pressure must be specified. Then:

$$\begin{aligned}\boldsymbol{F} &= \left(C_{\mathrm{x},j}\hat{\boldsymbol{x}} + C_{\mathrm{y},j}\hat{\boldsymbol{y}} + C_{\mathrm{z},j}\hat{\boldsymbol{z}}\right) q_j S = \left(C_{\mathrm{A},j}\hat{\boldsymbol{e}}_1 + C_{\mathrm{Y},j}\hat{\boldsymbol{e}}_2 + C_{\mathrm{N},j}\hat{\boldsymbol{e}}_3\right) q_j S \\ &= \left(C_{\mathrm{D,a}}\hat{\boldsymbol{D}}_\mathrm{a} + C_{\mathrm{S,a}}\hat{\boldsymbol{S}}_\mathrm{a} + C_{\mathrm{L,a}}\hat{\boldsymbol{L}}_\mathrm{a}\right) q_\mathrm{a} S = \left(C_{\mathrm{D,e}}\hat{\boldsymbol{D}}_\mathrm{e} + C_{\mathrm{S,e}}\hat{\boldsymbol{S}}_\mathrm{e} + C_{\mathrm{L,e}}\hat{\boldsymbol{L}}_\mathrm{e}\right) q_\mathrm{e} S\end{aligned} \tag{9}$$

The projection of the aerodynamic force in the apparent- and effective-velocity reference frames can be seen in Figure 2.

(We can also follow this non-dimensionalization for the aerodynamic torque acting on the kite in the kite-fixed reference frame: $\boldsymbol{\tau} = (C_\mathrm{l}\ b\ \hat{\boldsymbol{e}}_1 + C_\mathrm{m}\ c\ \hat{\boldsymbol{e}}_2 + C_\mathrm{n}\ b\ \hat{\boldsymbol{e}}_3)\ qS$).

2.7 the aerodynamic stability derivatives

Therefore, if we know functions determining the aerodynamic coefficients in one of these reference frames, we can determine the aerodynamic force $\boldsymbol{F}$. Stability derivatives - the series-expansion coefficients of these aerodynamic coefficients with respect to the angle-of-attack, side-slip angle, contol-surface deflections, and further relevant specified states - can be used to estimate the aerodynamic coefficients. This means that such a model is only valid when the expansion variables are close to their linearization point: zero.

For $i \in \{\mathrm{D}, \mathrm{S}, \mathrm{L}, \mathrm{l}, \mathrm{m}, \mathrm{n}\}$ and $j \in \{\mathrm{a}, \mathrm{e}\}$, we can use these stability derivatives to find the aerodynamic coefficients:

$$\begin{aligned} C_{i,j} \quad = \quad & C_{i,j_0} + \left(C_{i,j_\alpha}\, \alpha_j + C_{i,j_{\alpha^2}}\, \alpha_j^2 + C_{i,j_\beta}\, \beta_j + C_{i,j_{\beta^2}}\, \beta_j^2 \right) + \left(C_{i,j_p}\, p + C_{i,j_q}\, q + C_{i,j_r}\, r \right) \cdots \\ & + \left(C_{i,j_{\delta_\mathrm{a}}}\, \delta_\mathrm{a} + C_{i,j_{\delta_\mathrm{e}}}\, \delta_\mathrm{e} + C_{i,j_{\delta_\mathrm{r}}}\, \delta_\mathrm{r} \right) + \left(C_{i,j_{\delta_\mathrm{a}^2}}\, \delta_\mathrm{a}^2 + C_{i,j_{\delta_\mathrm{e}^2}}\, \delta_\mathrm{e}^2 + C_{i,j_{\delta_\mathrm{r}^2}}\, \delta_\mathrm{r}^2 \right) \cdots \\ & + \left(C_{i,j_{\alpha\delta_\mathrm{e}}}\, \alpha\delta_\mathrm{e} + C_{i,j_{\beta\delta_\mathrm{a}}}\, \beta\delta_\mathrm{a} + C_{i,j_{\beta\delta_\mathrm{r}}}\, \beta\delta_\mathrm{r} \right) + \text{any other expansion terms considered relevant} \end{aligned} \tag{10}$$

where δ_a is the aileron deflection, δ_e is the elevator deflection, δ_r is the rudder deflection, p is the roll rate, q is the pitch rate, and r is the yaw rate. These last three can be found as:

$$\begin{pmatrix} p \\ q \\ r \end{pmatrix} = \frac{1}{2} \begin{pmatrix} b & 0 & 0 \\ 0 & c & 0 \\ 0 & 0 & b \end{pmatrix} \frac{\boldsymbol{\omega}}{\left\| \boldsymbol{u}_j \right\|_2}. \tag{11}$$

Since the arguments of this series-expansion are (generally) distinct per reference velocity, it is only possible to determine the aerodynamic force if the reference velocity is explicitly known.

As an example, if we have used the effective velocity to define the aerodynamic coefficients:

$$\boldsymbol{F} = \left(C_{\mathrm{D,e}}\left(\alpha_\mathrm{e}, \beta_\mathrm{e}, ...\right) \hat{\boldsymbol{D}}_\mathrm{e} + C_{\mathrm{S,e}}\left(\alpha_\mathrm{e}, \beta_\mathrm{e}, ...\right) \hat{\boldsymbol{S}}_\mathrm{e} + C_{\mathrm{L,e}}\left(\alpha_\mathrm{e}, \beta_\mathrm{e}, ...\right) \hat{\boldsymbol{L}}_\mathrm{e} \right) q_\mathrm{e} S, \tag{12}$$

then (unless we're in the specific situation where the effective velocity is equivalent to the apparent velocity), we will not get the same force vector by applying the apparent velocity:

$$\boldsymbol{F} \neq \left(C_{\mathrm{D,e}}\left(\alpha_\mathrm{a}, \beta_\mathrm{a}, ...\right) \hat{\boldsymbol{D}}_\mathrm{a} + C_{\mathrm{S,e}}\left(\alpha_\mathrm{a}, \beta_\mathrm{a}, ...\right) \hat{\boldsymbol{S}}_\mathrm{a} + C_{\mathrm{L,e}}(\alpha_\mathrm{a}, \beta_\mathrm{a}, ...) \hat{\boldsymbol{L}}_\mathrm{a} \right) q_\mathrm{a} S. \tag{13}$$

Since stability derivatives give the recipe for generating these aerodynamic coefficients, **it is very important that the user specifies the corresponding reference velocity!**

3 determining the aerodynamic force

Our goal is to use the definitions described in the previous section to actually determine the aerodynamic force acting on a kite. As mentioned before, the method of determining this force depends on the reference velocity corresponding to the stability derivatives. We can roughly break the decision tree into three cases:

- (Section 3.1) without an induction model;
- (Section 3.2) with an induction model and the effective velocity as the corresponding reference velocity; and
- (Section 3.3) with an induction model and the apparent velocity as the corresponding reference velocity.

In this section, we will consider our modelled universe within the kite-fixed reference frame. Like this, we know that $\hat{\boldsymbol{e}}_1' = (1,0,0)^\top$, $\hat{\boldsymbol{e}}_2' = (0,1,0)^\top$, and $\hat{\boldsymbol{e}}_3' = (0,0,1)^\top$. We're also going to assume that we have an implicit function $\boldsymbol{f}_\mathrm{i}(\boldsymbol{u}_\mathrm{i};\cdot) = \boldsymbol{0}$ that constains the induced velocity according to the desired induction model, and will be described in another document.

3.1 without an induction model

If we chose not to model induction, then we effectively assume that $\boldsymbol{u}_\mathrm{i} = \boldsymbol{0}$. This means that the apparent and effective velocities must be equal: $\boldsymbol{u}_\mathrm{a} = \boldsymbol{u}_\mathrm{e}$. In this case, we can determine the angle-of-attack and side-slip angles with the equivalent expressions (3) and (6). Now, we can just drop these angles into (9) and (10) to give us the force and torque.

3.2 with an induction model, using the effective velocity as reference velocity

With an induction model, we know the effective velocity of the kite according to (4), because $\boldsymbol{u}_\mathrm{i}$ is constrained by our induction function $\boldsymbol{f}_\mathrm{i}(\boldsymbol{u}_\mathrm{i};\cdot) = \boldsymbol{0}$. As such, we can find the relevant angle-of-attack and side-slip angle with (6). Then, the force and moment can be found in a straight-forwards manner with (9) and (10), where $j = \mathrm{e}$.

(Notice, that when the force is projected within the effective velocity reference frame, the drag projection will not include any induced drag component. Neither, in this case, will the lift projection have been decreased by a not-occuring-in-this-case rotation about the induced angle of attack. That is to say: in this lucky case, we do not need to concern ourselves with any potential double-counting of the induction effect that might be present within the stability derivatives. The ideas in this comment will be expanded on in the following subsection 3.3.)

3.3 with an induction model, using the apparent velocity as reference velocity

Here, we have a more complicated scenario, though it make take a moment to explain the difficulty.

The aerodynamic force is generated by pressure differences in the fluid passing over a wetted body. That is, the aerodynamic force is generated by the effective velocity that is *actually* experienced along the surface of the body. However, in many circumstances, this force is projected according to the apparent velocity, because the apparent velocity may be known more reliably than the effective velocity itself. This happens - for example - when the forces are measured on a model that is placed in a wind-tunnel, where the experimenter knows the calibration of the wind-tunnel velocity (apparent velocity) but not necessarily the local velocity (effective velocity). This also happens in virtual wind tunnel simulations, where an apparent velocity is prescribed as an input, and the effective velocity is returned as part of the output.

This means that the projection reference frame is rotated by α_i away from the effective velocity reference frame. This generally, for positive α_i, has the effect that $L_\mathrm{a} \leq L_\mathrm{e}$ and $D_\mathrm{a} \geq D_\mathrm{e}$. (This increase to the apparent drag $(D_\mathrm{a}\hat{\boldsymbol{D}}_\mathrm{a} - D_\mathrm{e}\hat{\boldsymbol{D}}_\mathrm{e})$ is called the *induced drag*, which explains why there is no induced drag included in the forces when projected according to the effective velocity, as claimed in the previous section.)

Now, the difficulty is that stability derivatives corresponding to apparent velocities are necessarily based on a specific induced velocity field. And, there will be a significantly different induced velocity field if the kite is flying alone in a roughly-steady and roughly-level flight path, than if the kite is flying along a multi-kite trajectory with a tight radius, because the vorticity distribution in each case will be significantly different.

(As a limitting case, these situations will approach one another as the flight radius approaches infinity.)

That is to say, when the stability derivatives are determined according to the apparent velocity of a kite flying alone along a roughly-level path, $\boldsymbol{u}_{\text{a,alone}} = \boldsymbol{u}_{\text{e}} - \boldsymbol{u}_{\text{i,alone}}$, we cannot directly apply the apparent velocity from the multi-kite scenario to find the aerodynamic force and torque. We need to make a rough guess of what $\boldsymbol{u}_{\text{a,alone}}$ would correspond to the effective velocity in the multi-kite scenario:

$$\boldsymbol{u}_{\text{a,alone}} = \boldsymbol{u}_{\infty} - \dot{\boldsymbol{q}}_{\text{K}} + \boldsymbol{u}_{\text{i,mawes}} - \boldsymbol{u}_{\text{i,alone}}, \tag{14}$$

where $\boldsymbol{u}_{\text{i,mawes}}$ is the induced velocity consistent with the implicit induction function $\boldsymbol{f}_{\text{i}}(\boldsymbol{u}_{\text{i,mawes}}; \cdot) = \boldsymbol{0}$, and $\boldsymbol{u}_{\text{i,alone}}$ is the yet unknown approximation of the induced velocity for the kite flying alone with the given effective velocity.

(The ability to add and subtract (a.k.a. *superpose*) induced velocity fields is the greatest strength of potential flow models. This is valid as long as the flow is approximately inviscid and incompressible, with the further assumption of a modelled vorticity distribution that approximates reality, as the flow is roughly irrotational wherever the modelled vorticity is zero. Practically speaking, this limits the applicability of this superposition to sub-sonic cases where the boundary layer is thin, and the flow is fully attached. Since these criteria anyways describe the region of linearization for the stability derivatives, the superposition appears to be reasonable.)

In order to use $\boldsymbol{u}_{\text{a,alone}}$ to determine the angle-of-attack, side-slip angle, stability derivatives, and dynamic pressure that are needed to determine the aerodynamic force in (9), our goal is now to determine $\boldsymbol{u}_{\text{i,alone}}$.

In this subsection, we will describe:

- (Section 3.3.1) the effective velocity based on known angles,
- (Section 3.3.2) the modelled vorticity distribution for the kite flying alone,
- (Section 3.3.3) a numerical approximation for the resulting induced velocity,
- (Section 3.3.4) the implicit equation that constrains the aerodynamic force as a function of the induced velocity, and
- (Section 3.3.5 a rough estimate of the uncertainty in the induced velocity as a result of the modelled vorticity distribution.

3.3.1 the effective velocity according to defining angles

We know that the the effective velocity $\boldsymbol{u}_{\text{e}}$ can be described by the effective angle-of-attack and side-slip angle α_{e} and β_{e} as:

$$\hat{\boldsymbol{u}}_{\text{e}} = \left(\frac{1}{\sqrt{\tan^2\alpha_{\text{e}} + \sec^2\beta_{\text{e}}}}\right)\hat{\boldsymbol{e}}'_1 + \left(\frac{\tan\beta_{\text{e}}}{\sqrt{\tan^2\alpha_{\text{e}} + \sec^2\beta_{\text{e}}}}\right)\hat{\boldsymbol{e}}'_2 + \left(\frac{\tan\alpha_{\text{e}}}{\sqrt{\tan^2\alpha_{\text{e}} + \sec^2\beta_{\text{e}}}}\right)\hat{\boldsymbol{e}}'_3, \quad \boldsymbol{u}_{\text{e}} = u_{\text{e}}\hat{\boldsymbol{u}}_{\text{e}} \tag{15}$$

Qe can now compute the dynamic pressure q_{e}, as well as determine the projection directions of the drag and lift force $\hat{\boldsymbol{D}}_{\text{e}}$ and $\hat{\boldsymbol{L}}_{\text{e}}$, as described in Section 2.6.

3.3.2 vorticity distribution

If this kite is flying alone, in a flight path that is roughly steady and level, the vorticity distribution within our modelled universe might be approximated as a single horse-shoe vortex.[2] (This assumption is discussed in more detail in Section 3.3.5.) We will consider the nodes of this horse-shoe vortex to be

[2] A horse-shoe vortex is a classic vortex ring, where it is understood that the "closing" side of the horse-shoe vortex is sufficiently far away from the observation point, that its Biot-Savart influence can be safely neglected.

convected rigidly according to the effective velocity. This gives us the positions $\boldsymbol{x}_{\mathrm{w},i}$ of the four corners of our horse-shoe vortex, where $i = 1, ...4$. These positions read as:

$$\boldsymbol{x}_{\mathrm{w},1} = \boldsymbol{x}_{\mathrm{w},2} + \boldsymbol{u}_{\mathrm{e}} t_\infty, \qquad \boldsymbol{x}_{\mathrm{w},2} = -\frac{1}{2} b \hat{\boldsymbol{e}}_2, \qquad \boldsymbol{x}_{\mathrm{w},3} = \frac{1}{2} b \hat{\boldsymbol{e}}_2, \qquad \boldsymbol{x}_{\mathrm{w},4} = \boldsymbol{x}_{\mathrm{w},3} + \boldsymbol{u}_{\mathrm{e}} t_\infty, \tag{16}$$

where t_∞ is a "sufficiently long time" and with the limitting case $t_\infty \to \infty$.

You can see the assumed vorticity distribution in Figure 3.

We want to compute the induced velocity $\boldsymbol{u}_{\mathrm{i}}$ at the origin of our reference frame - the mid-span of the lifting-line - based on an unknown vortex strength Γ. For this, we apply the (known) analytical integral of the Biot-Savart[1] expression over straight vortex filaments, for each of the three filaments of the horse-shoe vortex:

$$\boldsymbol{u}_{\mathrm{i}} = \lim_{t_\infty \to \infty, \epsilon \to 0} \sum_{i=1}^{3} \boldsymbol{u}_{\mathrm{f}}(\boldsymbol{O}_{\mathrm{K}}, \boldsymbol{x}_{\mathrm{w},i}, \boldsymbol{x}_{\mathrm{w},i+1}, \Gamma, \epsilon) \tag{17}$$

$$\boldsymbol{u}_{\mathrm{f}}(\boldsymbol{x}_{\mathrm{o}}, \boldsymbol{x}_{\mathrm{w},i}, \boldsymbol{x}_{\mathrm{w},j}, \Gamma, \epsilon) = \frac{\Gamma}{4\pi} \left(\boldsymbol{r}_i \times \boldsymbol{r}_j \right) \frac{r_i + r_j}{r_i r_j \left(r_i r_j + \boldsymbol{r}_i^\top \boldsymbol{r}_j \right) + (\epsilon r_0)^2}, \tag{18}$$

$$\boldsymbol{r}_i = \boldsymbol{x}_{\mathrm{o}} - \boldsymbol{x}_{\mathrm{w},i}, \qquad r_i = \|\boldsymbol{r}_i\|_2 \tag{19}$$

$$\boldsymbol{r}_j = \boldsymbol{x}_{\mathrm{o}} - \boldsymbol{x}_{\mathrm{w},j}, \qquad r_j = \left\|\boldsymbol{r}_j\right\|_2 \tag{20}$$

$$\boldsymbol{r}_0 = \boldsymbol{x}_{\mathrm{w},j} - \boldsymbol{x}_{\mathrm{w},i}, \qquad r_0 = \|\boldsymbol{r}_0\|_2 . \tag{21}$$

You can see a sketch of how the vortices induce a velocity field in Figure 3; the tangential-direction velocity induced by a filament, computed by $\boldsymbol{u}_{\mathrm{f}}(\cdot)$, is shown in Figure 4.

Applying the above limits of steady convection ($t_\infty \to \infty$) with a vanishing regularization term ($\epsilon \to 0$), we find that:

$$\boldsymbol{u}_{\mathrm{i}} = \left(\frac{\Gamma \sin\alpha_{\mathrm{e}} \cos\alpha_{\mathrm{e}} \sqrt{\tan^2\alpha_{\mathrm{e}} + \sec^2\beta_{\mathrm{e}}}}{\pi b} \right) \hat{\boldsymbol{e}}'_1 - \left(\frac{\Gamma \cos^2\alpha_{\mathrm{e}} \sqrt{\tan^2\alpha_{\mathrm{e}} + \sec^2\beta_{\mathrm{e}}}}{\pi b} \right) \hat{\boldsymbol{e}}'_3. \tag{22}$$

(As a brief sanity-check: you might notice that, in the case of no apparent side-slip ($\beta_{\mathrm{e}} = 0$), this induction is equivalent to the small-angle approximation of the induction due to two semi-infinite, 2D vortices at a distance of a half-span from the observation point. That is:

$$\boldsymbol{u}_{\mathrm{i}}|_{\beta_{\mathrm{e}}=0} = \left(\frac{\Gamma}{2\pi} \right) \left(\frac{b}{2} \right)^{-1} \left(\frac{\hat{\boldsymbol{e}}'_2 \times \hat{\boldsymbol{u}}_{\mathrm{e}}}{\left\|\hat{\boldsymbol{e}}'_2 \times \hat{\boldsymbol{u}}_{\mathrm{e}}\right\|_2} \right) \Bigg|_{\beta_{\mathrm{e}}=0} = \frac{\Gamma}{b\pi} \left(\hat{\boldsymbol{e}}'_2 \times \hat{\boldsymbol{u}}_{\mathrm{e}} \right) \Big|_{\beta_{\mathrm{e}}=0} .)$$

3.3.3 numerical approximations to the induced velocity

Any constraint with as many trigonometric functions as (22) will be a nightmare to our solver, so let's make a series expansion with respect to the angles, and then use a small-angle-approximation to drop

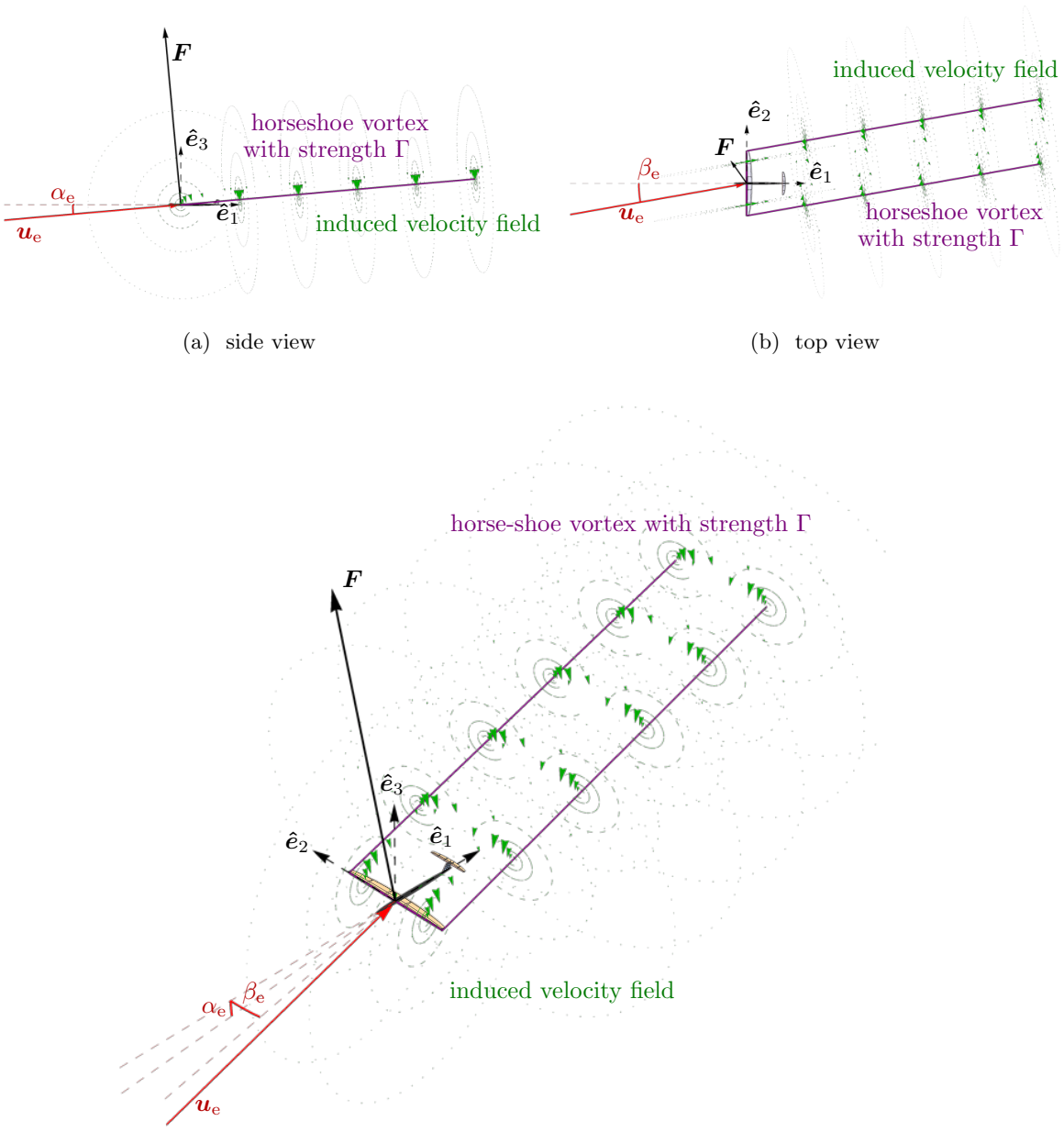

(a) side view

(b) top view

(c) isometric view

Figure 3: We model the vorticity distribution, for the kite flying alone along a roughly-level flight path with non-zero effective angle of attack α_e and effective side-slip angle β_e, as a horse-shoe vortex. The filaments of this vortex induce a circulating velocity field, which can be superposed (as sketched in green). The strength of the induced velocity is indicated by the length of the green dashes. The strength of the induced velocity is proportional to the lift-force in the effective velocity reference frame, according to the Kutta-Joukowski expression (29).

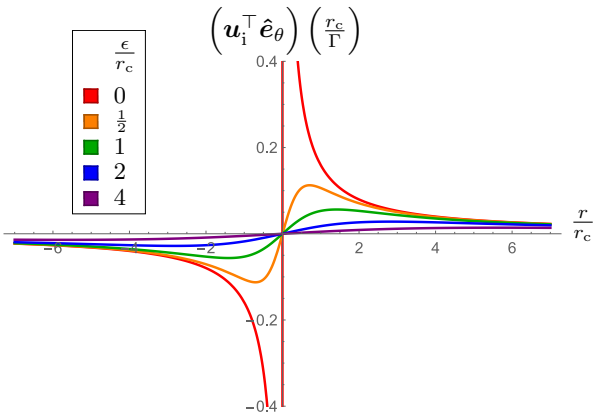

Figure 4: The (non-dimensional) tangential direction induced velocity as related to the cut-off radius ϵ, here shown proportional to a particular vortex core radius r_c, and the distance r between the vortex and the observation point. In particular, we consider here a 2D vortex (infinitely long), according to the regularized straight-filament Biot-Savart expression $\boldsymbol{u}_\mathfrak{f}(\cdot)$. Notice that when $\epsilon = 0$, the induced velocity is discontinuous at the position of the vortex center. With a non-zero cut-off radius, we have a smooth induced velocity field, but under-estimations in the magnitude of the induction.

the higher order terms:

$$\widetilde{\boldsymbol{u}}_\mathrm{i}^{A,B} = \sum_{a=0}^{A}\sum_{d=0}^{B}\left(\frac{\partial^d}{\partial\beta_\mathrm{e}^d}\left(\frac{\partial^a \boldsymbol{u}_\mathrm{i}}{\partial\alpha_\mathrm{e}^a}\right)\bigg|_{\alpha_\mathrm{e}=0,\beta_\mathrm{e}=0}\frac{\alpha_\mathrm{e}^a}{a!}\frac{\beta_\mathrm{e}^d}{d!}\right) \tag{23}$$

$$\widetilde{\boldsymbol{u}}_\mathrm{i}^{1,1} = \frac{\Gamma}{\pi b}\left(\alpha_\mathrm{e}\hat{\boldsymbol{e}}_1' - \hat{\boldsymbol{e}}_3'\right) \tag{24}$$

$$\widetilde{\boldsymbol{u}}_\mathrm{i}^{1,2} = \frac{\Gamma}{\pi b}\left(\left(\frac{1}{2}\alpha_\mathrm{e}\left(2+\beta_\mathrm{e}^2\right)\right)\hat{\boldsymbol{e}}_1' - \left(1+\frac{1}{2}\beta_\mathrm{e}^2\right)\hat{\boldsymbol{e}}_3'\right) \tag{25}$$

$$\widetilde{\boldsymbol{u}}_\mathrm{i}^{2,1} = \frac{\Gamma}{\pi b}\left(\alpha_\mathrm{e}\hat{\boldsymbol{e}}_1' + \left(\frac{1}{2}\left(-2+\alpha_\mathrm{e}^2\right)\right)\hat{\boldsymbol{e}}_3'\right) \tag{26}$$

$$\widetilde{\boldsymbol{u}}_\mathrm{i}^{2,2} = \frac{\Gamma}{\pi b}\left(\left(\frac{1}{2}\alpha_\mathrm{e}\left(2+\beta_\mathrm{e}^2\right)\right)\hat{\boldsymbol{e}}_1' + \left(\frac{1}{4}\left(-2\left(2+\beta_\mathrm{e}^2\right)+\alpha_\mathrm{e}^2\left(2+3\beta_\mathrm{e}^2\right)\right)\right)\hat{\boldsymbol{e}}_3'\right). \tag{27}$$

If we expect that the effective angle-of-attack and side-slip angles would remain in the range[3] ($-10° \leq \alpha_\mathrm{e} \leq 25°$) and ($-20° \leq \beta_\mathrm{e} \leq 20°$), we can find the maximum error introduced by the truncation of this series expansion:

$$\varepsilon_\mathrm{trunc}^{A,B} = \frac{\left\|\widetilde{\boldsymbol{u}}_\mathrm{i}^{A,B} - \boldsymbol{u}_\mathrm{i}\right\|_2}{\left\|\boldsymbol{u}_\mathrm{i}\right\|_2} \tag{28}$$

Descriptive values of this truncation error are reported in Table 1.

In Section 3.3.5, we will use this truncation error to decide which numerical approximation $\widetilde{\boldsymbol{u}}_\mathrm{i}^{A,B}$ to implement in the `awebox`. In the meantime, let's see how this numerical approximation will be used in the `awebox`.

[3] here, rounded up from those values suggested for the Ampyx AP2

$\max_{\alpha_e,\beta_e} \varepsilon^{A,B}_{\text{trunc}}$	$A=1$	$A=2$
$B=1$	9.5%	6.0%
$B=2$	10.3%	1.8%

(a) maximum truncation error in range

$\overline{\varepsilon^{A,B}_{\text{trunc}}}$	$A=1$	$A=2$
$B=1$	2.5%	2.0%
$B=2$	2.5%	0.3%

(b) average truncation error in range

Table 1: Descriptive values of the truncation error $\epsilon^{A,B}_{\text{trunc}}$ within the range of $(-10° \leq \alpha_e \leq 25°)$ and $(-20° \leq \beta_e \leq 20°)$. This truncation error **does not include modelling-assumption errors** as resulting from the assumptions, such as the highly simplistic assumed vorticity distribution, and should not be regarded as complete.

3.3.4 the resulting implicit equation

We would now like to know the magnitude of that vortex strength Γ. We'll find this vortex strength with the Kutta-Joukowski relationship:

$$\boldsymbol{F}^\top \hat{\boldsymbol{L}}_e = \boldsymbol{F}^\top \left(\frac{\boldsymbol{u}_e \times \hat{\boldsymbol{e}}'_2}{\left\| \boldsymbol{u}_e \times \hat{\boldsymbol{e}}'_2 \right\|_2} \right) = b\rho\Gamma \left\| \boldsymbol{u}_e \times \hat{\boldsymbol{e}}'_2 \right\|_2 \quad \Rightarrow \quad \Gamma = \boldsymbol{F}^\top \left(\boldsymbol{u}_e \times \hat{\boldsymbol{e}}'_2 \right) \left(\frac{1}{b\rho \left\| \boldsymbol{u}_e \times \hat{\boldsymbol{e}}'_2 \right\|_2^2} \right), \tag{29}$$

giving us a strength Γ that can be used in (23) to approximate the induced velocity.

We now have everything we need to determine the apparent velocity in the alone-flying case via (14). If we combine (3), (9), (10), (23) and (29) we construct an implicit equation that constrains the aerodynamic force:

$$\boldsymbol{F} = \boldsymbol{F}\left(\boldsymbol{u}_{\text{a,alone}}\left(\boldsymbol{u}_e, \boldsymbol{F} \right) \right). \tag{30}$$

Remember that, within this section, we have described our universe within the kite-fixed reference frame, and that we need to apply the direction-cosine-matrix $\underline{\boldsymbol{R}}_K$ to return to the earth-fixed reference frame.

3.3.5 estimating the modelling uncertainty

Let's make a little pause to guess how much uncertainty in (22) is a result of the simple vorticity distribution model applied here.

The vorticity distribution along the span of the kite is highly uncertain, with imputs completely outside the scope of the `awebox` in its present form. That is, the `awebox` has no knowledge of the specific placement of the control surfaces whose deflection will cause sharp changes in the spanwise distribution of lift over the wing. Nor does the `awebox` have any knowledge of the sectionwise airfoil profiles that make up the kites wings; the specific placement of any onboard propellors or turbines; or any other local kite geometric information that would make a "reasonable" recontruction of the spanwise lift or circulation[4] distribution possible.

In order, then, not to pretend more accuracy than actually possible, we have chosen here to make the most simplistic vorticity distribution available - the single horseshoe vortex described above. But, we might like to guess the order-of-magnitude of the resulting uncertainty.

To make this guess, let's suppose that we had chosen a more optimistic[5], but still simple vorticity distribution: the elliptic circulation distribution that results from an elliptic lift distribution. In this case, we can find the induced velocity $\boldsymbol{u}_{\text{i,elliptic}}$ at our observation point $\boldsymbol{O}_K$ by integrating the induction

[4] Circulation is defined as the flux of vorticity through a surface S with unit normal vector $\hat{\boldsymbol{n}}$: $\Gamma = \iint_S \boldsymbol{\omega} \cdot \hat{\boldsymbol{n}} \, \mathrm{d}S$. Circulation has units [m^2/s]. In lifting line models, where the only vorticity bound to the surface is modelled by vortex filaments laying on the lifting line, this circulation at some span-wise position is equivalent to the "vortex strength" of the vortex filament that is sliced at this span-wise position. If we have a vortex surface (or sheet) rather than a vortex filament, then the strength γ [m/s] is the derivative of the circulation, along the direction of the sheet perpendicular to the vorticity's orientation.

[5] the ellipticial lift distribution is well known[2] to give the minimum induced drag effect

for the modelled vorticity distribution of semi-infinite vortex filaments extending from the lifting line, as convected infinitely far by the (constant) effective velocity:

$$\boldsymbol{u}_{\mathrm{i,elliptic}} = \lim_{t_\infty \to \infty, \epsilon \to 0} \int_{\zeta=-\frac{1}{2}}^{\zeta=\frac{1}{2}} \boldsymbol{u}_{\mathrm{f}}(\boldsymbol{O}_{\mathrm{K}}, \boldsymbol{x}_{\mathrm{w,elliptic},0}\left(\zeta\right), \boldsymbol{x}_{\mathrm{w,elliptic},\infty}\left(\zeta\right), \frac{\partial \Gamma_{\mathrm{elliptic}}}{\partial \zeta}\left(\zeta\right), \epsilon)\, \mathrm{d}\zeta \tag{31}$$

$$\boldsymbol{x}_{\mathrm{w,elliptic},0}\left(\zeta\right) = \zeta b \hat{\boldsymbol{e}}_2, \qquad \boldsymbol{x}_{\mathrm{w,elliptic},\infty}\left(\zeta\right) = \boldsymbol{x}_{\mathrm{w,elliptic},0}\left(\zeta\right) + \boldsymbol{u}_{\mathrm{e}} t_\infty, \tag{32}$$

where ζ is the non-dimensional spanwise position, stretching from $\zeta = -\frac{1}{2}$ at the wingtip furthest towards $-\hat{\boldsymbol{e}}_2$, and $\zeta = +\frac{1}{2}$ at the wingtip furthest towards $+\hat{\boldsymbol{e}}_2$. To save space, we have here not explicitly written the contribution of the bound vortices, which would vanish as the regularization term ϵ itself vanishes.

Further, we need to switch the direction of the trailing vortices, by using the sign of the vortex sheet strength $\frac{\partial \Gamma_{\mathrm{elliptic}}}{\partial \zeta}$, which is positive for $\zeta > 0$ so that the direction of the vorticity is analogous to that in the horseshoe vortex wake node numbering of (16).

Finally, we can use two facts to determine the vortex sheet strength $\frac{\partial \Gamma_{\mathrm{elliptic}}}{\partial \zeta}(\zeta)$. First, the spanwise circulation distribution $\Gamma_{\mathrm{elliptic}}(\zeta)$ should be elliptical, with a maximum circulation Γ_{max} at the mid-span ($\zeta = 0$). Second, the integral of the Kutta-Joukowski expression must still give us the same lift L_{e} that we have determined the kite to be experiencing. From this information, we find that:

$$\frac{\partial \Gamma_{\mathrm{elliptic}}}{\partial \zeta} = 4\Gamma_{\mathrm{max}} \frac{\zeta}{\sqrt{1-\zeta^2}}, \qquad \Gamma_{\mathrm{max}} = \frac{4L_{\mathrm{e}}}{b\pi\rho u_{\mathrm{e}}} \left(\cos\alpha_{\mathrm{e}}\right) \sqrt{\sec^2\beta_{\mathrm{e}} + \tan^2\alpha_{\mathrm{e}}} \tag{33}$$

If we put together the above information, and evaluate the integral (31), we find the induced velocity predicted by an elliptical circulation distribution.

$$\boldsymbol{u}_{\mathrm{i,elliptic}} = \left(\frac{4L_{\mathrm{e}} \sin\alpha_{\mathrm{e}} \cos^2\alpha_{\mathrm{e}} \left(\tan^2\alpha_{\mathrm{e}} + \sec^2\beta_{\mathrm{e}}\right)}{3\pi b^2 \rho u_{\mathrm{e}}} \right) \hat{\boldsymbol{e}}_1 - \left(\frac{4L_{\mathrm{e}} \cos^3\alpha_{\mathrm{e}} \left(\tan^2\alpha_{\mathrm{e}} + \sec^2\beta_{\mathrm{e}}\right)}{3\pi b^2 \rho u_{\mathrm{e}}} \right) \hat{\boldsymbol{e}}_3. \tag{34}$$

If we use this alternate possibility of the induced velocity, we can estimate the amount of uncertainty in our model - that purely arises due to the uncertain vorticity distribution

$$\varepsilon_{\mathrm{m}} = \frac{\left\| \boldsymbol{u}_{\mathrm{i,elliptic}} - \boldsymbol{u}_{\mathrm{i}} \right\|_2}{\left\| \boldsymbol{u}_{\mathrm{i}} \right\|_2} = \frac{1}{3}, \tag{35}$$

which is to say that we estimate the modelling uncertainty on the induced velocity, to be on the order of 33%. With this sort of uncertainty, it would make sense to value the linearity of $\widetilde{\boldsymbol{u}_{\mathrm{i}}}^{1,1}$ more than the small truncation error of $\widetilde{\boldsymbol{u}_{\mathrm{i}}}^{2,2}$, and it is $\widetilde{\boldsymbol{u}_{\mathrm{i}}}^{1,1}$ which is implemented in the `awebox`.

4 code options

Our goal is to describe how an `awebox` user can interact with the code, specifically with respect to the kite aerodynamic models.

Specifically, the user might interact with the kite aerodynamics for topics pertaining to:

- (Section 4.1) the kite geometry,
- (Section 4.2) the stability derivatives applied to the kite, and
- (Section 4.3) the reference velocity of the stability derivatives.

4.1 the kite geometry

The user can interact with the information about the kite geometry in the kite data python file. For example, the default kite model is the Ampyx AP2, with a kite data python file `awebox/opts/kite_data/ampyx_data.py`. Within this file is a function called `geometry()`, where the user has the option of specifying the geometric parameters of the kite.

4.2 the stability derivatives

The user can interact with the information about the stability derivatives in the kite data python file. For example, the default kite model is the Ampyx AP2, with a kite data python file `awebox/opts/kite_data/ampyx_data.py`. Within this file is a function called `aero_deriv()`, where the user has the option of specifying the aerodynamic stability derivatives of the kite.

4.3 the reference velocity

As previously mentioned, it is necessary to specify the velocity used to define the aerodynamic coefficients. In the `awebox`, the user can make this specification with `options['model']['aero']['aero_coeff_ref_velocity']` which can be set to either:

- `'app'`, the apparent velocity, as typically used when the coefficients are determined according to well-defined external flows. This is typical of wind-tunnel model tests, or computer-simulationed "virtual" wind-tunnel tests. It is important to specify that this option is based on the apparent velocity of a single kite, flying in roughly steady and level conditions.
- `'eff'`, the effective velocity, as typically used when the coefficients are determined according to well-defined effective flow measurements, and the external flow is uncertain. This might occur during a test flight campaign, where the reference velocity is that velocity measured by the Pitot tube. This option is the default option in the `awebox`.

The `awebox` gives, as outputs, predictions of the aerodynamic coefficients at any point along the trajectory. These coefficients correspond to the effective velocity experienced at that point in the trajectory.

5 Conclusion

In this document, we have described the method for modelling the aerodynamic force on a kite, as used in the `awebox`.

We have seen that there is a large difference in the modelling method depending on which reference velocity is chosen for the stability derivatives.

From this, we conclude that the user should take care that their selection from among the user options best fits their requirements.

References

[1] E. Branlard. Wind turbine aerodynamics and vorticity-based methods : fundamentals and recent applications. Springer, Roskilde, Denmark, 2017.

[2] J. Katz and A. Plotkin. Low-speed aerodynamics. Cambridge University Press, Cambridge, UK, 2 edition, 2010.